

Supporting Information

High performance solution-processed green phosphorescent organic light-emitting diodes with high current efficiency and long-term stability

Athithan Maheshwaran,^a Vijaya Gopalan Sree,^a Ho-Yeol Park,^a Woosum Cho,^a Hyein Kim,^a Raja Kumaresan,^a Youngkwang Kim,^b Jae Chol Lee,^b Myungkwan Song,^{c*} and Sung-Ho Jin,^{a*}

A. Maheshwaran, Dr. V. G. Sree, H. Kim, H.-Y. Park, Dr. W. Cho, H. Kim, R. Kumaresan, Prof. S.-H. Jin

^aDepartment of Chemistry Education, Graduate Department of Chemical Materials, Institute for Plastic Information and Energy Materials, Pusan National University, Busandaehakro 63-2, Busan 46241, Republic of Korea

E-mail: shjin@pusan.ac.kr

Y. Kim, Dr. J. C. Lee

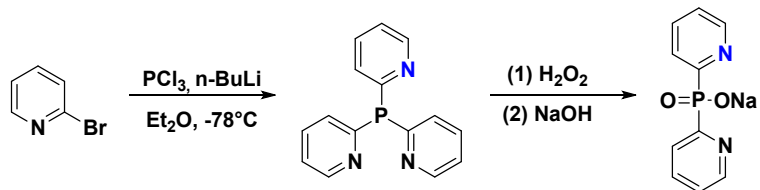
^bLG Display E6 Block LG Science Park 30, Magokjungang 10-ro, Gangseo-gu, Seoul 07796, Republic of Korea

Dr. M. Song

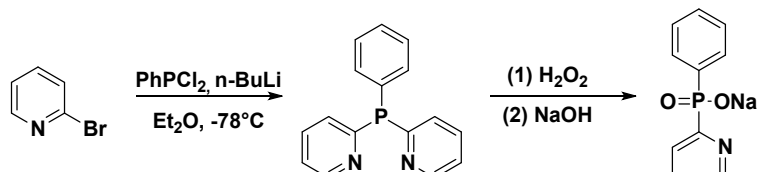
^cAdvanced Functional Thin Films Department Surface Technology Division Korea Institute of Materials Science (KIMS) 797 Changwondaero, Changwon, Gyeongnam 51508, Republic of Korea E-mail: smk1017@kims.re.kr

Theoretical Computation

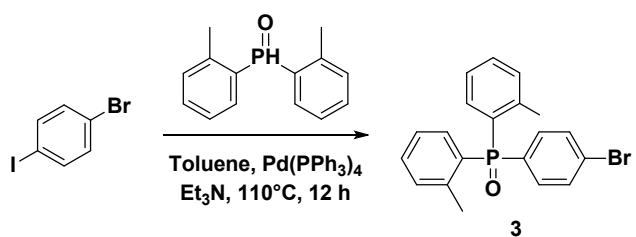
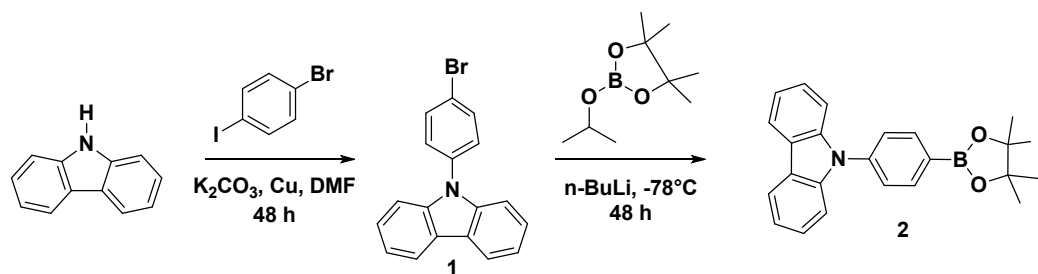
DFT calculations were performed for both Ir(III) complexes and host molecules. Non-metal atoms of C, H, N, F, P and O were described by the all-electron basis set of B3LYP/6-31G (d). The effective core potentials with a B3LYP/LanL2DZ basis set were used for Ir atoms. Both ground and excited state calculations were performed for all molecules. The excitation behaviors of the complexes were computed by time-dependent DFT (TD-DFT) method based on optimized geometries at the ground states. All calculations were carried out by using the Gaussian 09 program.



sym

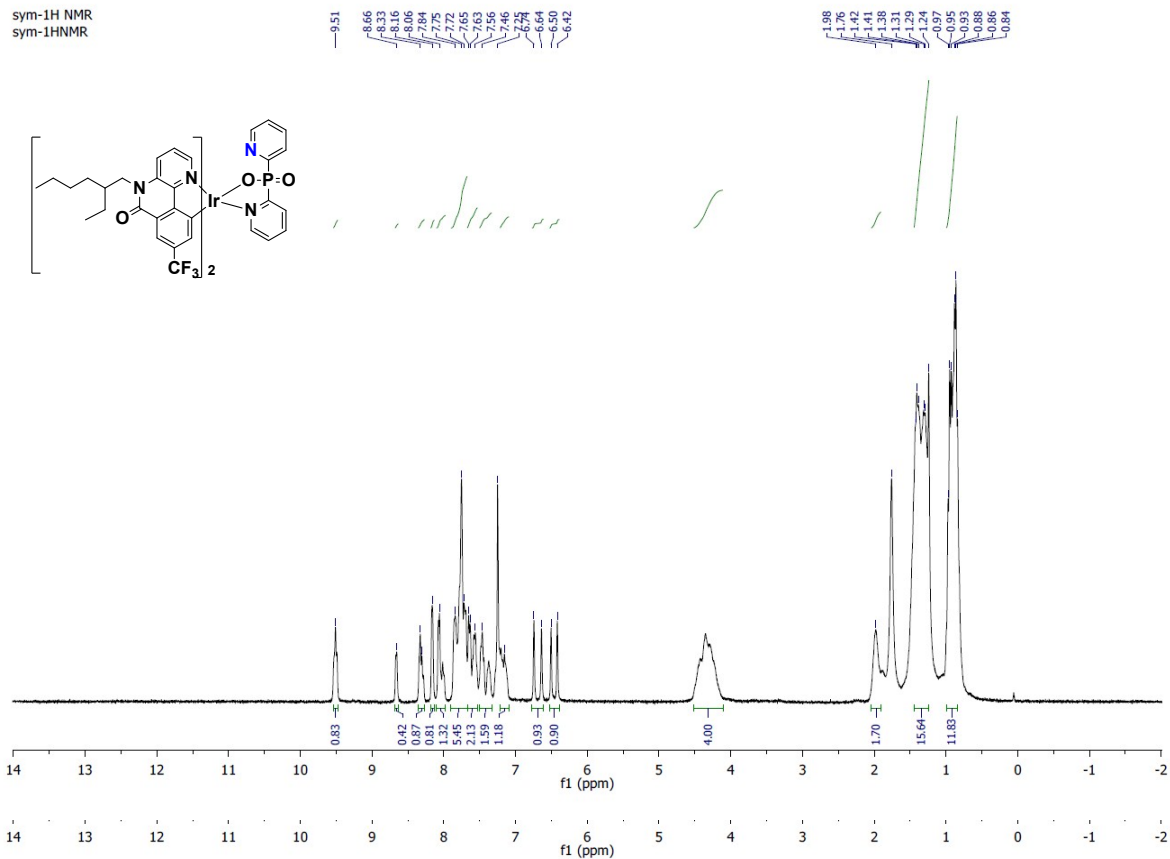


asym

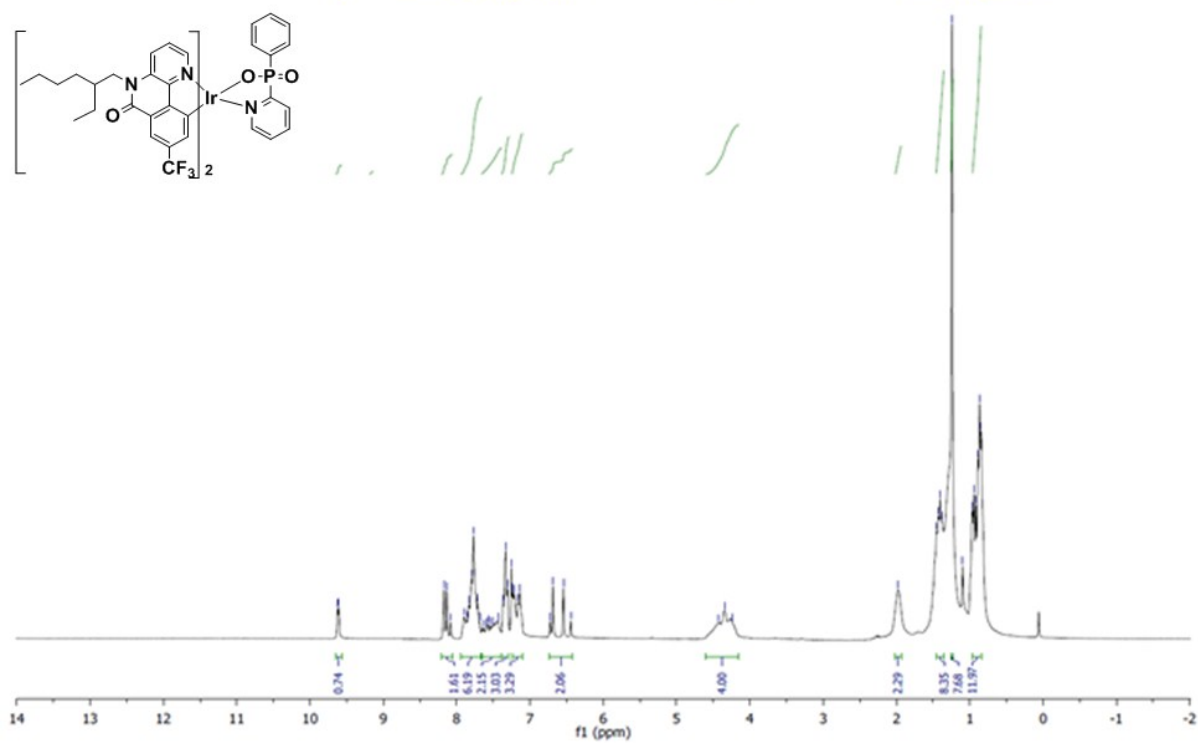


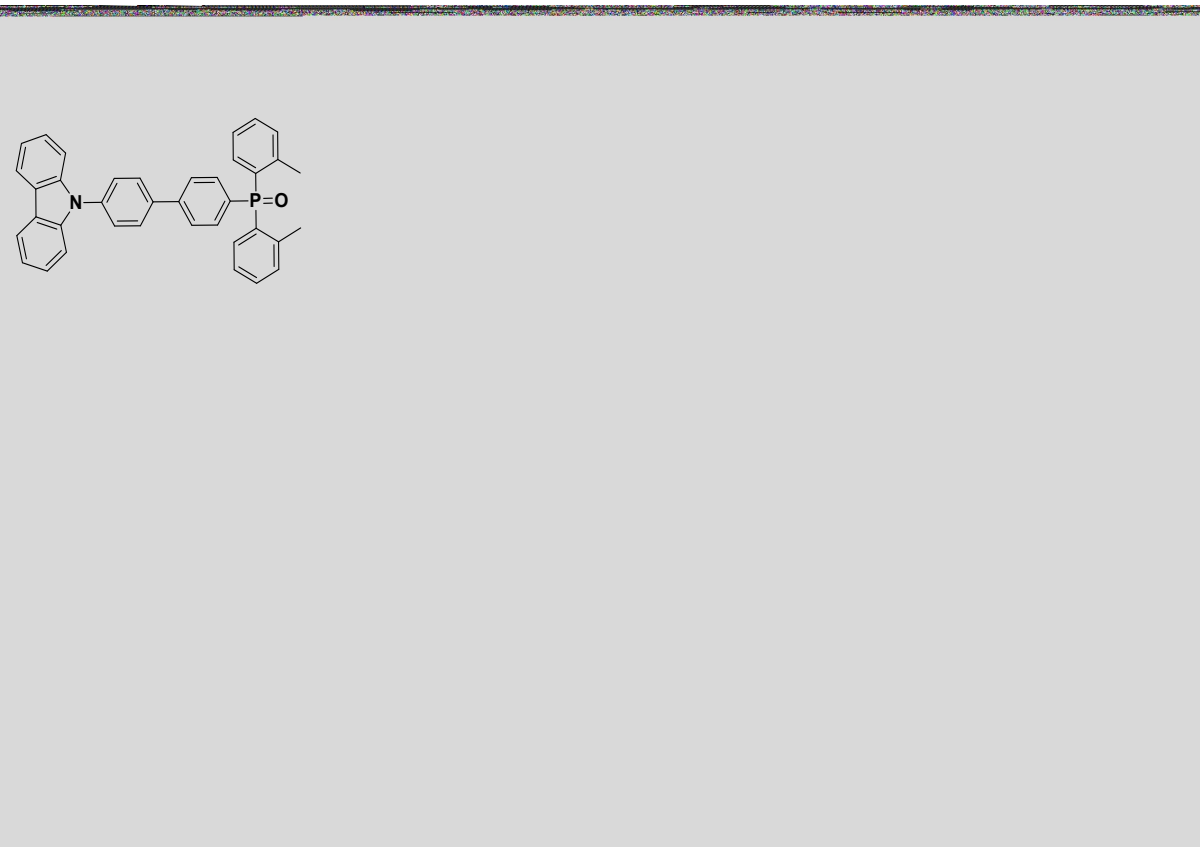
Scheme S1. Synthetic routes of ancillary ligands and *m*-CBPPO1 intermediates.

sym-¹H NMR
sym-¹HNMR

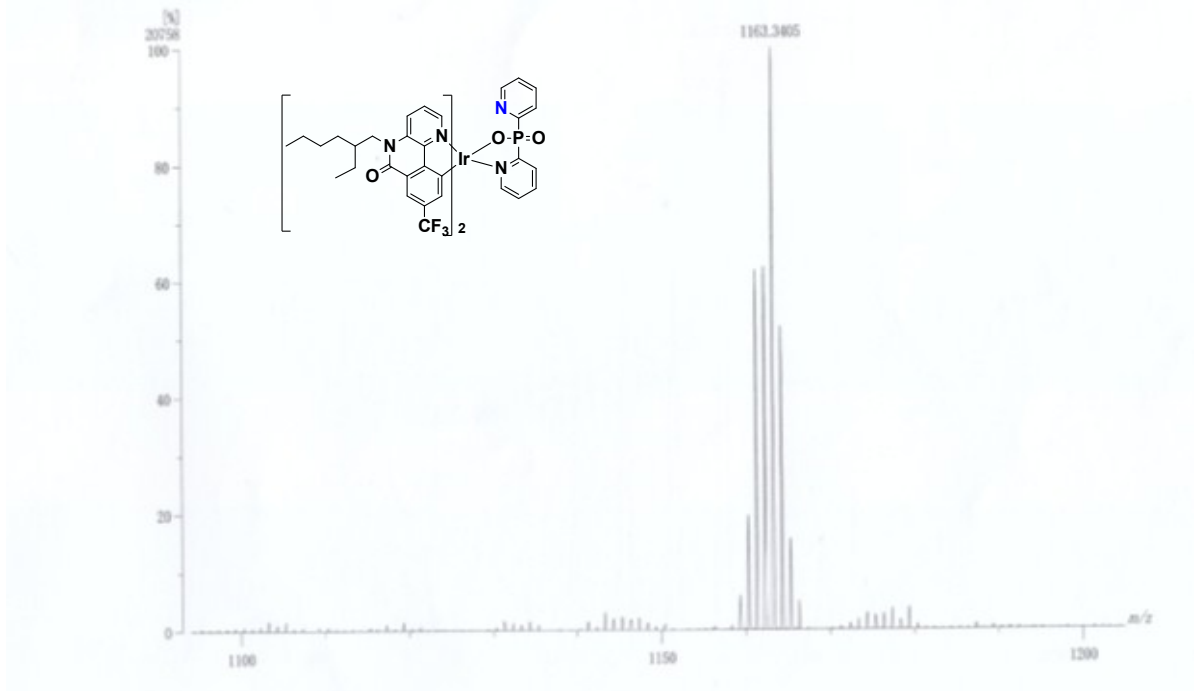


asym-1HNMR
asym-1HNMR





[Mass Spectrum]
Data : Sym-C32H53F9-NB04P-HRFAE Date : 12-Sep-2018 10:34
Instrument : MDstar
Sample : -
Inlet: Direct Ion Mode: FAB+
Spectrum Type: Normal Ion [EF-Linear]



[Mass Spectrum]
Data : Asym-CS363FBrNCO4P-HRFAB Date : 12-Sep-2018 10:38
Instrument : MSstation
Sample : ~
Inlet : Direct Ion Mode : FAB+
Spectrum Type : Normal Ion [EF-Linear]

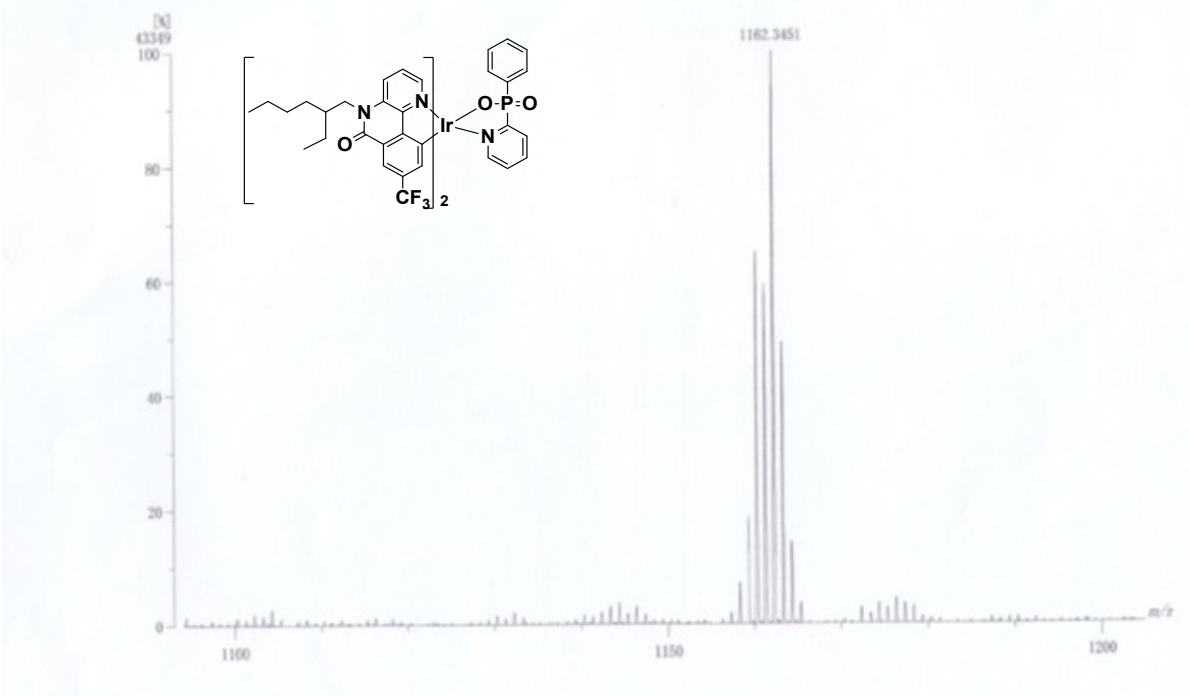
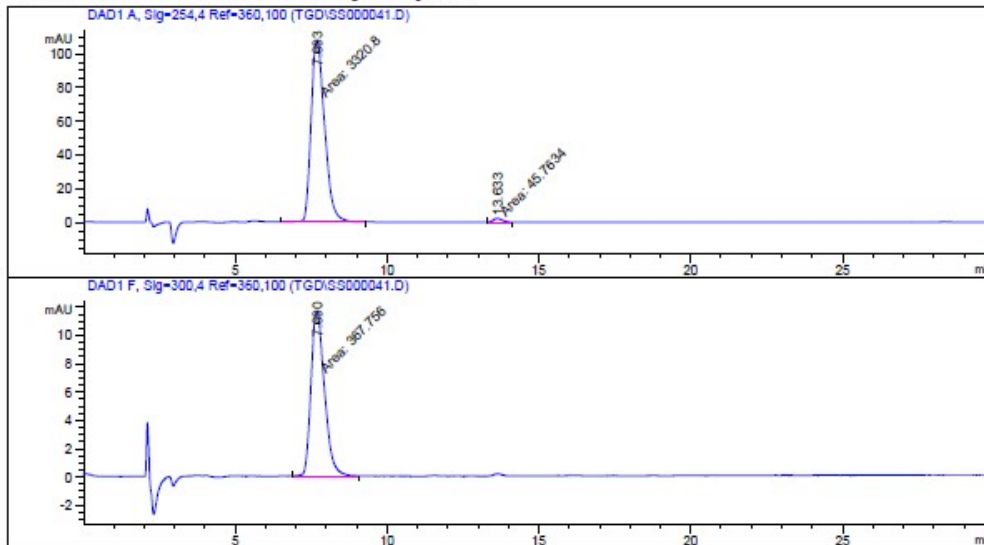


Fig. S1. ^1H NMR and mass spectra of sym-Ir1, asym-Ir2 and *m*-CBPP01.

Sample Info : Ir (dpp)

Additional Info : Peak(s) manually integrated



=====
=====
Area Percent Report
=====
=====

Sorted By : Signal
Multiplier: : 1.0000
Dilution: : 1.0000
Use Multiplier & Dilution Factor with ISTDs

Signal 1: DAD1 A, Sig=254,4 Ref=360,100

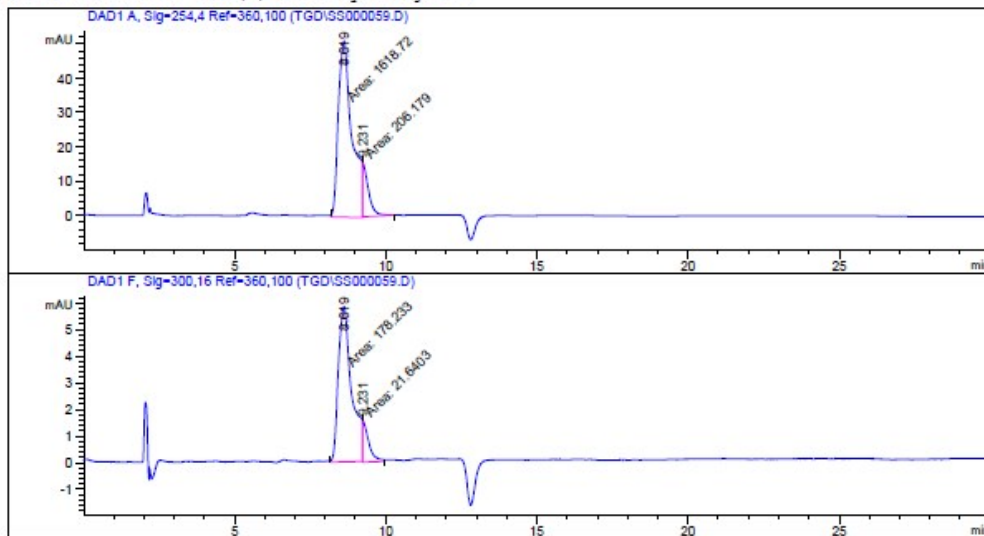
Peak #	RetTime [min]	Type	Width [min]	Area [mAU*s]	Height [mAU]	Area %
1	7.693	MM	0.5155	3320.80127	107.87209	98.6407
2	13.633	MM	0.3373	45.7637	2.26142	1.3593
Totals :				3366.56464	109.63352	

Signal 2: DAD1 F, Sig=300,4 Ref=360,100

Peak #	RetTime [min]	Type	Width [min]	Area [mAU*s]	Height [mAU]	Area %
1	7.690	MM	0.5243	367.75620	11.69084	100.0000
Totals :				367.75620	11.69084	

Sample Info : Ir(ppy) in THF

Additional Info : Peak(s) manually integrated



=====
Area Percent Report
=====

Sorted By : Signal
Multiplier: : 1.0000
Dilution: : 1.0000
Use Multiplier & Dilution Factor with ISTDs

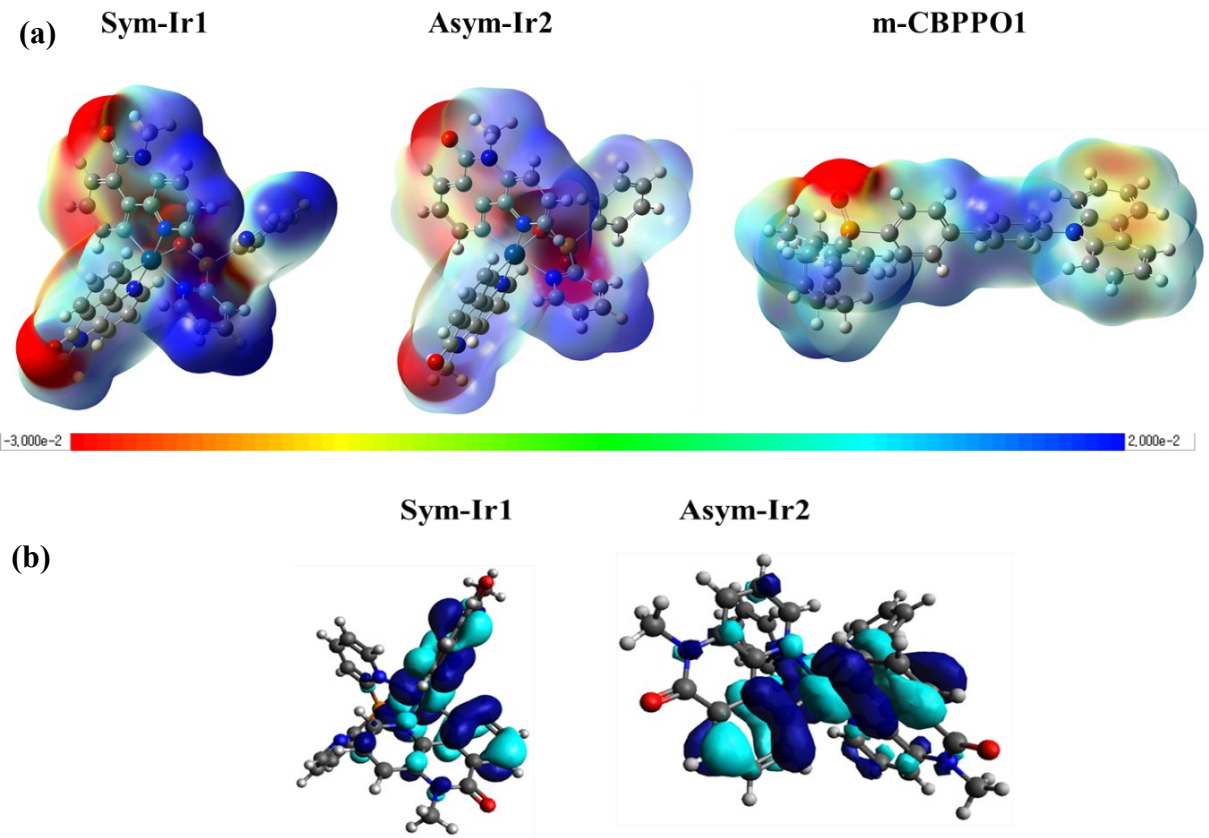
Signal 1: DAD1 A, Sig=254,4 Ref=360,100

Peak #	RetTime [min]	Type	Width [min]	Area [mAU*s]	Height [mAU]	Area %
1	8.619	MM	0.5269	1618.72363	51.20451	88.7019
2	9.231	MM	0.2130	206.17944	16.13075	11.2981
Totals :				1824.90308	67.33526	

Signal 2: DAD1 F, Sig=300,16 Ref=360,100

Peak #	RetTime [min]	Type	Width [min]	Area [mAU*s]	Height [mAU]	Area %
1	8.619	MM	0.5102	178.23302	5.82273	89.1730
2	9.231	MM	0.2253	21.64027	1.60097	10.8270
Totals :				199.87329	7.42370	

Fig. S2. HPLC chromatograms of sym-Ir1 and asym-Ir2.



g. S3. (a) Calculated electrostatic surface potentials of Ir(III) complexes and *m*-CBPPO1 and, (b) E_T state visualization of sym-Ir1 and asym-Ir2 complexes.

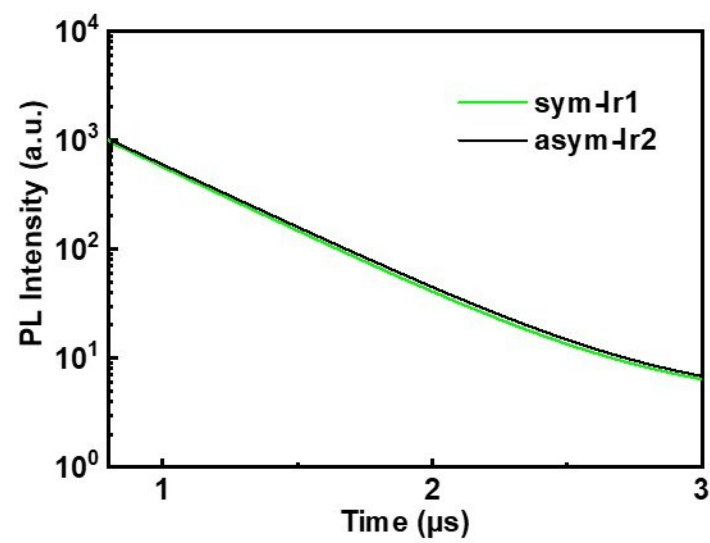


Fig. S4. PL decay curves measured for sym-Ir1 and asym-Ir2 in CH_2Cl_2 solution ($1 \times 10^{-4}\text{M}$) upon N_2 purging.

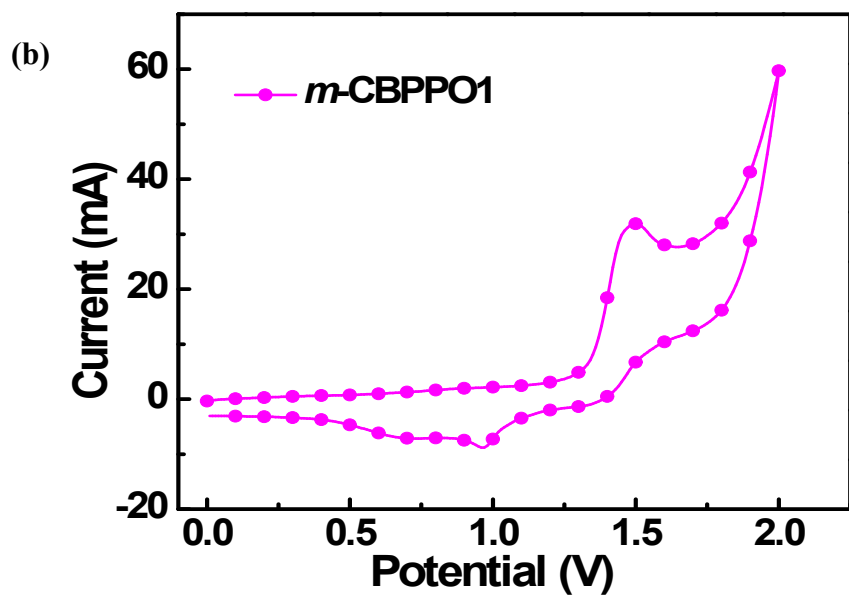
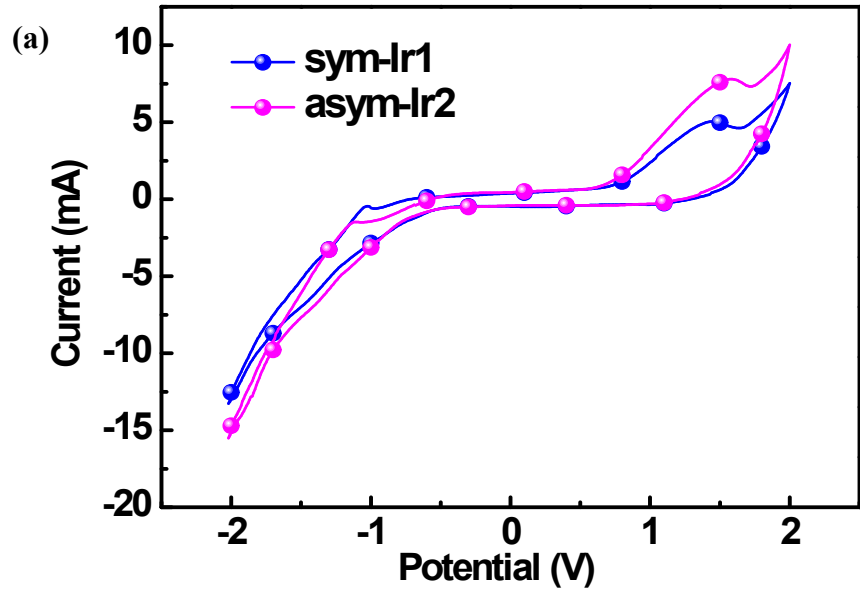


Fig. S5. Cyclic voltammograms of (a) sym-Ir1, asym-Ir2 and (b) *m*-CBPPO1.

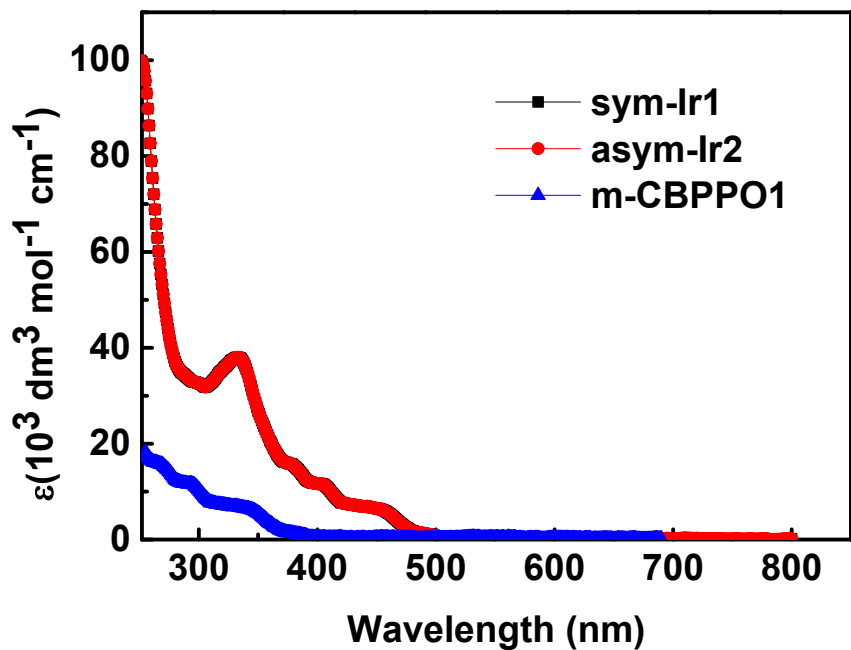


Fig. S6. Absorption coefficient spectra for sym-Ir1, asym-Ir2 and m-CBPPO1.

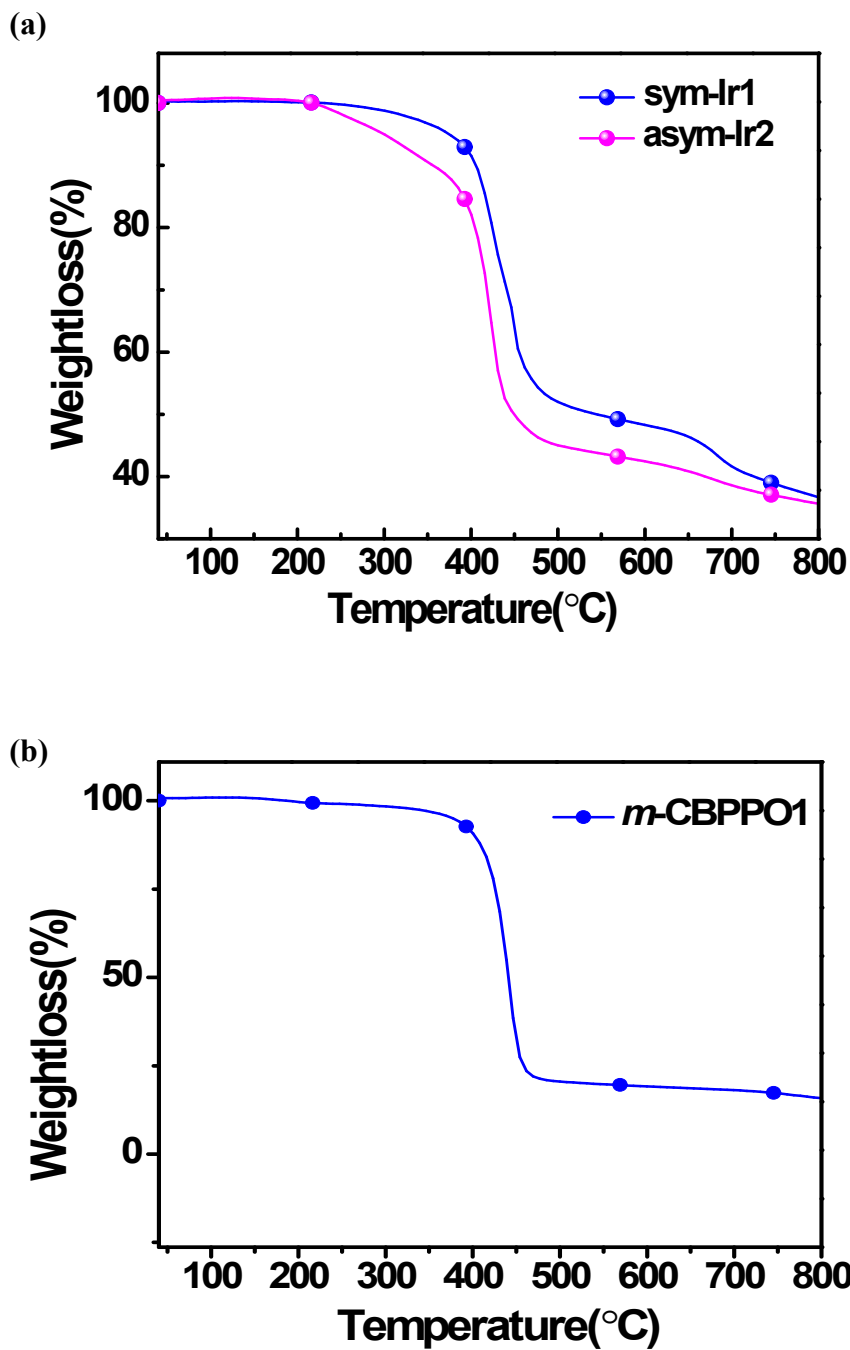


Fig. S7. TGA analysis of (a) sym-Ir1, asym-Ir2 and (b) *m*-CBPPO1.

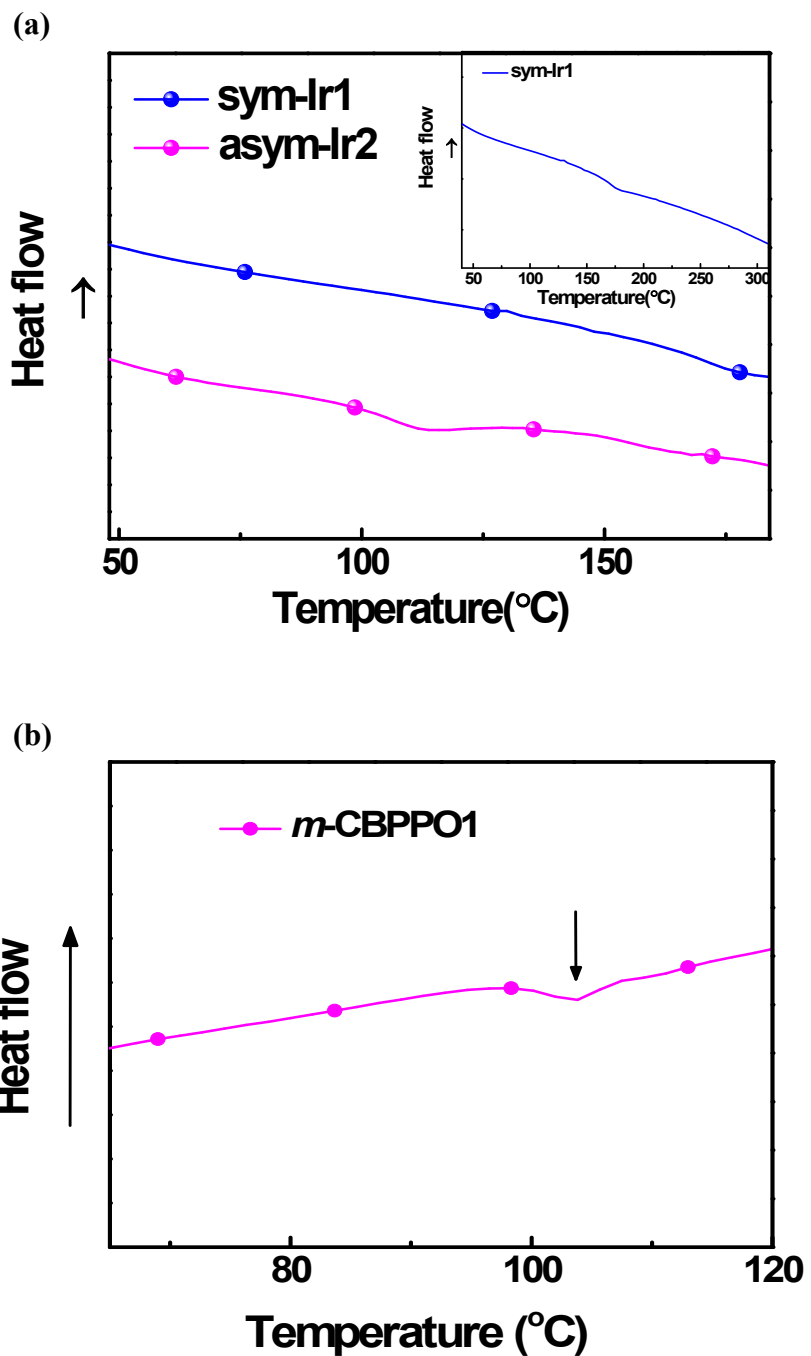


Fig. S8. DSC analysis of (a) sym-Ir1, asym-Ir2 (insert showing the T_g of sym-Ir1) and (b) *m*-CBPP01 at a heating rate of $10\text{ }^{\circ}\text{C min}^{-1}$.

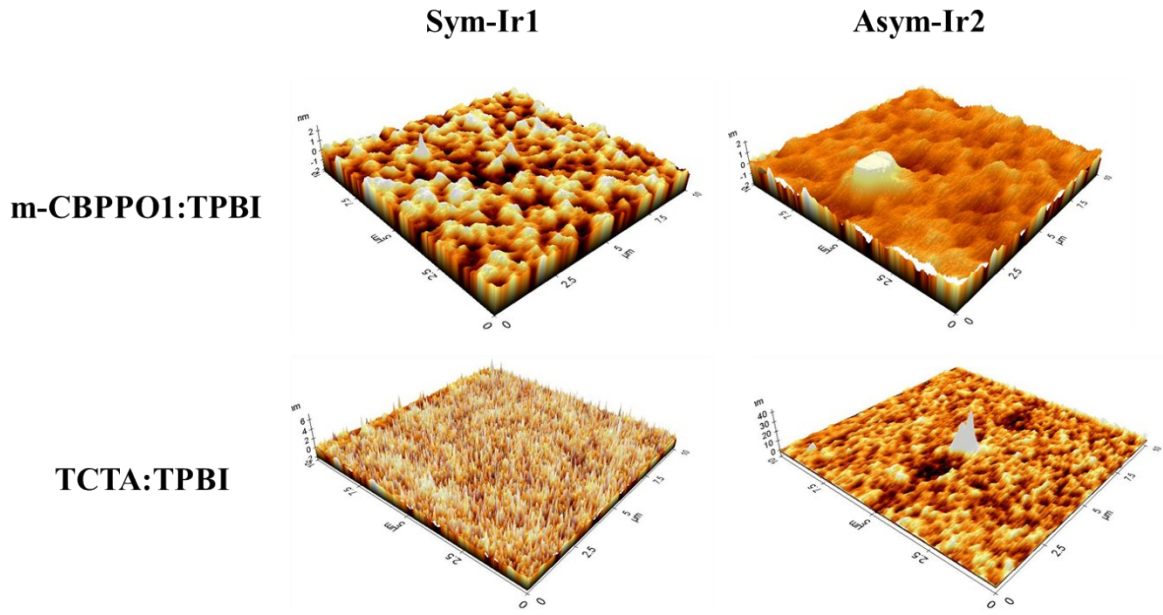


Fig. S9. Surface morphologies (3D images) of solution processed films.

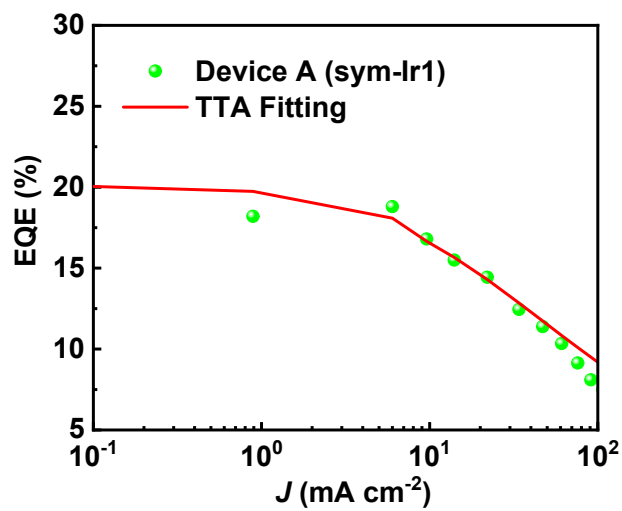
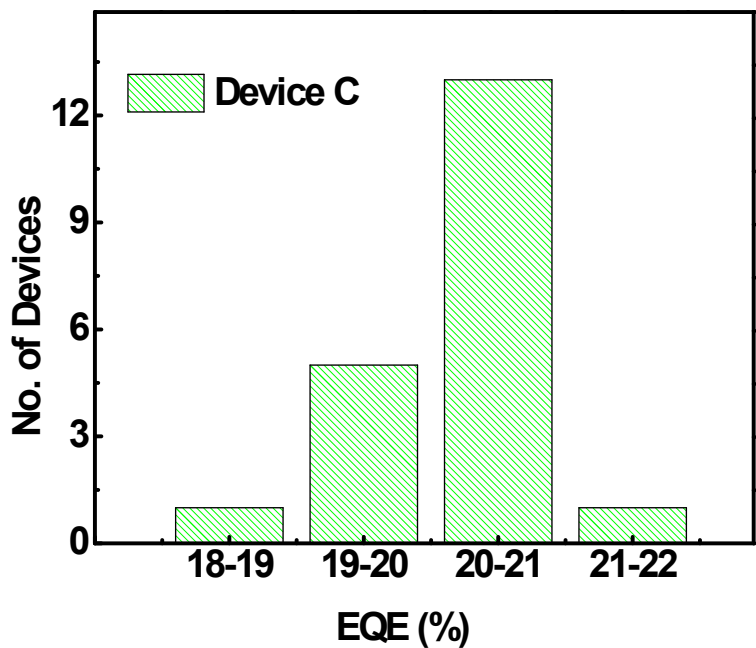


Fig. S10. EQE-current density (EQE- J) dependence of devices with complex sym-Ir1. The solid lines stand for the TTA fitting curve.

(a)



(b)

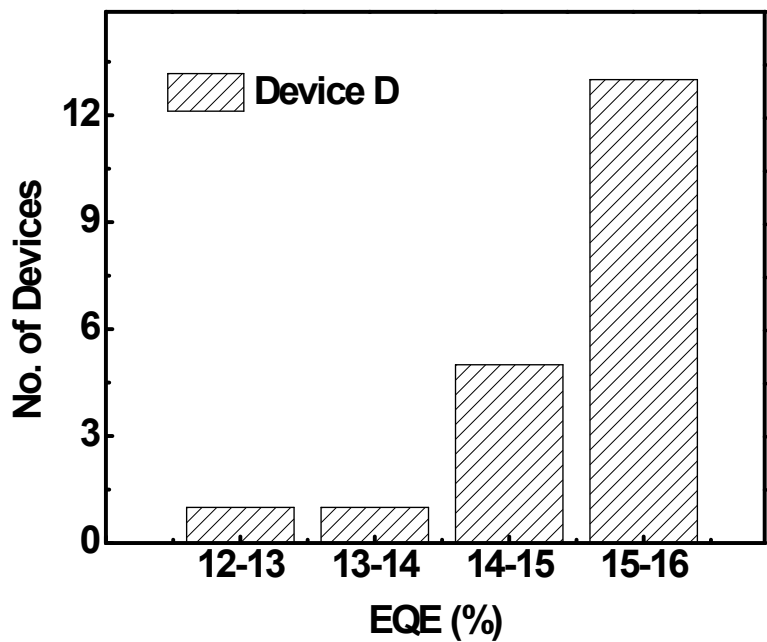


Fig. S11. Repeatability of the devices fabricated using the optimized structure using complexes (a) sym-Ir1 and (b) asym-Ir2.

Table S1 Literature summary of phosphine oxide functionalized Ir(III) complexes for PHOLEDs

Dopant	EQE _{max} (%)	CE _{max} (cd/A)	Device fabrication	Host	Reference
Sym-Ir1 (green)	20.82	68.72	Solution process	m-CBPPO1(New host) / TPBi	This work
Ir3 (green)	19.40	85.31	Solution-process	TCTA/TPBi	1
Ir2 (Deep-blue)	3.8	4.3	Vaccum-process	TSPO1	2
G2 (green)	19.8	60.6	Vaccum-process	-	3
DPP-2 (blue)	28.3	58.78	Vaccum-process	-	4
Ir-PO (green)	9.67	34.23	Vaccum-process	-	5
PO-Firpic (blue)	7.1	11.1	Solution-process	PVK/OXD	6
Ir(tfmppy) ₂ (tpip) (green)	-	67.95	Vaccum-process	mCP	7
G2 (green)	-	113.23	Vaccum-process	mCP	8
Ir(tfmppy) ₂ (tpip) (green)	21.9	83.53	Vaccum-process	D-QDPO (new host)	9
G4 (green)	-	50.8	Vaccum-process	SimCP2	10
G4 (green)	29.5	92.83	Vaccum-process	PPO21	11
Ir(dfptfmpm) tpip (green)	-	54.29	Vaccum-process	mCP	12

References

1. V. G. Sree, A. Maheshwaran, H. Kim, H-Y. Park, Y. Kim, J. C. Lee, M. Song, S-H. Jin, *Adv. Funct. Mater.*, 2018, **28**, 1804714.
2. G. Sarada, A. Maheshwaran, W. Cho, T. Lee, S. H. Han, J. Y. Lee, S-H. Jin, *Dyes Pigm.*, 2018, **150**, 8.
3. F. Zhang, W. Li, Y. Yu, Y. Jing, D. Ma, F. Zhang, S. Li, G. Cao, Z. Li, G. Guo, B. Wei, D. Zhang, L. Duan, C. Li, Y. Feng, B. Zhai, *J. Mater. Chem. C*, 2016, **4**, 5475.
4. Z-G. Wu, Y-M. Jing, G-Z. Lu, J. Zhou, Y-X. Zheng, L. Zhou, Y. Wang, Y. Pan, *Sci. Rep.* DOI: 10.1038/srep38478
5. G. Zhou, Q. Wang, C-L. Ho, W-Y. Wong, D. Ma, L. Wang, Z. Lin, *Chem. Asian J.*, 2008, **3**, 1841
6. C. Fan, Y. Li, C. Yang, H. Wu, J. Qin, Y. Cao, *Chem. Mater.*, 2012, **24**, 4587.
7. Y-C. Zhu, L. Zhou, H-Y. Li, Q-L. Xu, M-Y. Teng, Y-X. Zheng, J-L. Zuo, H-J. Zhang, X-Z. You, *Adv. Mater.*, 2011, **23**, 4046.
8. H-Y. Li, L. Zhou, M-Y. Teng, Q-L. Xu, C. Lin, Y-X. Zheng, J-L. Zuo, H-J. Zhang, X-Z. You, *J. Mater. Chem. C*, 2013, **1**, 565.
9. Z- G. Wu, J. Zhou, L. Yu, G. Karotsis, Y. Wang, Y-X. Zheng, Y. Pan, *J. Mater. Chem. C*, 2017, **5**, 8579.
10. Q-L. Xu, C-C. Wang, T-Y. Li, M-Y. Teng, S. Zhang, Y-M. Jing, X. Yang, W-N. Li, C. Lin, Y-X. Zheng, J-L. Zuo, X-Z. You, *Inorg. Chem.*, 2013, **52**, 4916.
11. H-B. Han, Z-L. Tu, Z-G. Wu, Y-X. Zheng, *Dyes Pigm.* DOI:10.1016/j.dyepi g.2018.09.017.
12. Y-H. Zhou, J. Xu, Z-G. Wu, Y-X. Zheng, *J. Organomet. Chem.*, 2017, **848**, 231.

Table S2. Theoretical calculation results for symmetric and asymmetric Ir(III) complexes.

Complex	State	λ_{cal} [nm]	f	Composition	Assignments
sym-Ir1	T1	504		H→L [92.7]	MLCT/LLCT/ $\pi\pi^*$
	S1		0.016	H→L [96.9]	MLCT/LLCT/ $\pi\pi^*$
asym-Ir2	T1	506		H→L [91.1]	MLCT/LLCT/ $\pi\pi^*$
	S1		0.009	H→L [97.2]	MLCT/LLCT/ $\pi\pi^*$

^aH→L represents the HOMO to LUMO transition. f stands for oscillator strength.

Table S3. Absorption coefficients for sym-Ir1, asym-Ir2 and m-CBPPO1.

Complex	absorption ^a	
	λ (nm)	$\{\epsilon, 10^3 \text{ L mol}^{-1} \text{ cm}^{-1}\}$
sym-Ir1	333 (38.1), 379 (15.4), 405 (11.4), 453 (6.2)	
sym-Ir2	334 (42.9), 404 (12.0), 454 (7.6)	
<i>m</i> -CBPPO1	293 (53.3), 319 (46.1)	

^aAbsorption measurements of complexes were taken in CH_2Cl_2 .

Time (Hours)	EQE_C (%)	EQE_D (%)	Luminance_C (cd m ⁻²)	Luminance_D (cd m ⁻²)
0	18.2	15.2	351.45	302.48
50	15.14	11.23	310.11	257.42
100	14.26	10.18	265.44	199.57
150	13.76	9.59	254.59	185.29
200	13.47	9.29	249.32	177.51
250	13.15	8.93	242.97	168.97
300	12.83	8.59	236.62	160.83
350	12.54	8.27	229.87	155.25
400	12.28	8.00	225.16	149.79

Table S4. EQE and luminance values for devices C and D at regular intervals.

Stability of the devices measured at 10 mA cm⁻².

